Journal of Zhejiang University SCIENCE A
ISSN 1673-565X (Print); ISSN 1862-1775 (Online)
www.zju.edu.cn/jzus; www.springerlink.com
E-mail: jzus@zju.edu.cn

Finite element modeling for analysis of cracked cylindrical pipes*

SUNG Wen-pei†1, GO Cheer-germ[2], SHIH Ming-hsiang[3]

([1]Department of Landscape Design and Management, National Chin-Yi University of Technology, Taiping, Taichung 41111, Taiwan, China)

([2]Department of Civil Engineering, National Chung Hsing University, Taichung 40227, Taiwan, China)

([3]Department of Construction Engineering, National Kaohsiung First University of Science and Technology, Kaohsiung 811, Taiwan, China)

†E-mail: sung809@ncut.edu.tw

Received Sept. 19, 2006; revision accepted Mar. 15, 2007

Abstract: The characteristic properties of shell element with similar shapes are used to generate a so-called super element for the analysis of the crack problems for cylindrical pressure vessels. The formulation is processed by matrix condensation without the involvement of special treatment. This method can deal with various singularity problems and it also presents excellent results to crack problems for cylindrical shell. Especially, the knowledge of the kind of singular order is not necessary in super element generation; it is very economical in terms of computer memory and programming. This method also exhibits versatility to solve the problem of kinked crack at cylindrical shell.

Key words: Crack shell, Super-element, Pressure vessel
doi:10.1631/jzus.2007.A1373 **Document code:** A **CLC number:** TB6; TK91

INTRODUCTION

Pressure vessels are loaded by surging and water hammering or summing up by both of these two. Conventionally, the design formulas for the determination of the thickness of cylindrical pressure vessels are based on two considerations: the hoop stress and the longitudinal stress. Thus, the requirements of minimum thickness and maximum allowable working internal pressure are inferred (JHGPA, 1986; Nichols, 1987; Ugural, 1981). However, the defect problems of material such as bumping damage and crack in the vessel may induce considerable flexibility and reduce the load carrying capacity and the tolerance of flaws (Shephard *et al.*, 1981; Chen and Lin, 1985; Atluri, 1986; Anderson, 1991; Hooton and Tomkins, 1996; Ainsworth *et al.*, 1992; Folias, 1999; Minnetyan and Chamis, 1999). The tolerance assessment of the existing crack is very important for the integrity of vessel. The evaluation of the stress intensity factors of a cylindrical shell with various crack orientations has been studied (Sih, 1977; Lakshminarayana *et al.*, 1982; Zheng *et al.*, 2006). Since there are mathematical complication and the limited capabilities of analytical tools, the numerical method of finite element approach provides a logical procedure to analyze the fracture tolerance by skipping the difficulties introduced by structural geometry and boundary conditions. However, the direct application of the finite element method to model stress variation in the vicinity of a crack tip requires the use of an extremely fine grid. Therefore, massive amount of element node means a great amount of computing time. It costs a great amount of computing memory and converges very slowly because of deficiencies in singularity representation (Knott, 1973; Kobayashi, 1973; Lynn and Ingraffen, 1978; Shephard *et al.*, 1981; Chen and Lin, 1985). In order to calculate effectively and generate better results, the super element constructed by embedding proper singular order has been considered instead of the ordinary method (Shephard *et al.*, 1981; Lynn and Ingraffen, 1978; Mutri *et al.*, 1985; Song, 2004). Nevertheless, the order of singularity for problems such as kinked crack and crack front in a 3D solid cannot be determined easily. This leads to the

* Project (No. NSC-95-2221-E-167-002) supported by the National Science Council of Taiwan, China

necessity of a general approach to deal with these kinds of problems (Dutta *et al.*, 1990; Le Van and Royer, 1986; Go and Lin, 1991; 1994; Go and Chen, 1992; Go *et al.*, 1998). Herein, a super element formulated by using the characteristic properties of stiffness matrix for the elements with similar shape is recommended to solve these problems. The concept of this method is to use a group of similar elements to generate layers until there is infinitely small around the singular point. The formulation is processed by matrix condensation without involvement of special treatment. This method can deal with any kind of singularity problems and present excellent results to crack problems for cylindrical shell.

MEMBRANE SHELL ELEMENTS

For a cylindrical pressure vessels shown in Fig.1a, the wall of this pressure vessel is thin, which thickness is less than one-tenth of the radius and it does not change abruptly. The wall is subjected to the stresses that distributed through the thickness uniformly (Timoshenko, 1955; Timoshenko and Woinowsky-Krieger, 1959; Pilkey, 1994). Thus the membrane theory (Timoshenko and Woinowsky-Krieger, 1959; Szilard, 1974), an assumption of the element without flexural rigidity and only carrying the lateral loads by axial

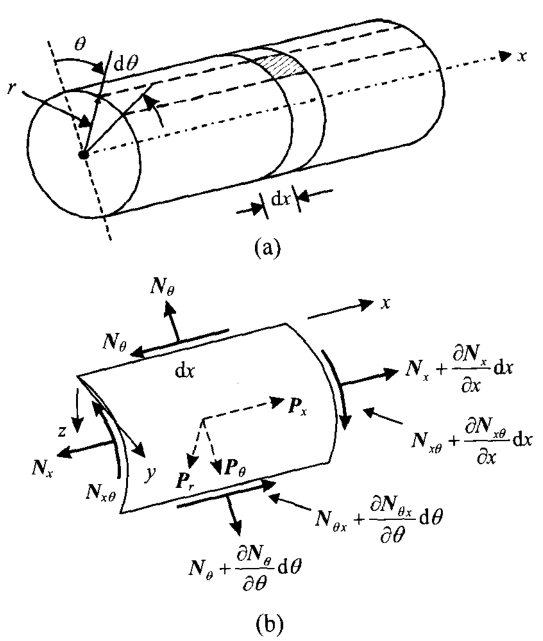

Fig.1 Cylindrical pressure vessel and membrane shell forces. (a) Cylinder; (b) Membrane shell forces

and transverse shear forces, is applied for the analysis. Based on the assumptions of elastic material and small displacement, it is reasonable to use the potential energy to develop a crack shell element. A free body diagram of membrane element including the forces is shown in Fig.1b. The coordinate x and the angle θ were used to describe the position of the shell element.

By the assumption of constant thickness shell, the nodal displacements u_i, v_i and w_i shown in the parent element are related to the membrane strains ε_x, ε_θ and $\gamma_{x\theta}$ on the material coordinates as (Cook *et al.*, 1989)

$$\begin{bmatrix} X \\ Y \\ Z \end{bmatrix} = \sum_{i=1}^{8} N_i(\xi,\eta) \begin{bmatrix} x_i \\ y_i \\ z_i \end{bmatrix}, \quad (1)$$

where $N_i(\xi, \eta)$ is the shape functions associated with the parent element. Accordingly, the related displacements are

$$\begin{bmatrix} U \\ V \\ W \end{bmatrix} = \sum_{i=1}^{8} N_i(\xi,\eta) \begin{bmatrix} u_i \\ v_i \\ w_i \end{bmatrix}, \quad (2)$$

and the three types of strains related to the displacements $\boldsymbol{u}$ are

$$\begin{bmatrix} \varepsilon_x \\ \varepsilon_\theta \\ \gamma_{x\theta} \end{bmatrix} = \begin{bmatrix} \frac{\partial N_i}{\partial x} & 0 & 0 \\ 0 & \frac{1}{r}\frac{\partial N_i}{\partial \theta} & -\frac{N_i}{r} \\ \frac{1}{r}\frac{\partial N_i}{\partial \theta} & \frac{\partial N_i}{\partial x} & 0 \end{bmatrix} \begin{bmatrix} u_i \\ v_i \\ w_i \end{bmatrix}. \quad (3)$$

Eq.(3) may be denoted as $\boldsymbol{\varepsilon}=\boldsymbol{Bu}$.

The relationship for stresses-strains is $\boldsymbol{\sigma}=\boldsymbol{D\varepsilon}$, where

$$\boldsymbol{D} = \begin{bmatrix} E_{xx} & E_{x\theta} & 0 \\ E_{\theta x} & E_{\theta\theta} & 0 \\ 0 & 0 & G_{x\theta} \end{bmatrix}.$$

The stiffness matrix $\boldsymbol{K}$ and force matrix $\boldsymbol{Q}$ are formulated as:

$$\boldsymbol{K}=t\iint \boldsymbol{B}^{\mathrm{T}}\boldsymbol{DB}r\mathrm{d}x\mathrm{d}\theta=t\int_{-1}^{1}\int_{-1}^{1}\boldsymbol{B}^{\mathrm{T}}\boldsymbol{DB}\det|\boldsymbol{J}|\,r\mathrm{d}\xi\mathrm{d}\eta, \quad (4)$$

$$\boldsymbol{Q}=\iint \boldsymbol{P}^{\mathrm{T}}\boldsymbol{q}r\mathrm{d}x\mathrm{d}\theta=\int_{-1}^{1}\int_{-1}^{1}\boldsymbol{P}^{\mathrm{T}}\boldsymbol{q}\det|\boldsymbol{J}|\,r\mathrm{d}\xi\mathrm{d}\eta, \quad (5)$$

where $\boldsymbol{J}$ is Jacobian matrix and can be shown as

$$\boldsymbol{J}=\begin{bmatrix}\dfrac{\partial x}{\partial \xi} & \dfrac{\partial \theta}{\partial \xi}\\ \dfrac{\partial x}{\partial \eta} & \dfrac{\partial \theta}{\partial \eta}\end{bmatrix}=\begin{bmatrix}\cdots\dfrac{\partial N_i}{\partial \xi}\cdots\\ \cdots\dfrac{\partial N_i}{\partial \eta}\cdots\end{bmatrix}\begin{bmatrix}\vdots & \vdots\\ x_i & \theta_i\\ \vdots & \vdots\end{bmatrix}. \quad (6)$$

In Eqs.(4) and (5), matrices $\boldsymbol{B}$ and $\boldsymbol{J}$ are functions of ξ and η, the symbols t and r represent the thickness and the radius of cylindrical shell element respectively.

STIFFNESS FOR SIMILAR SHELL ELEMENT

For two similar elements with ratio α, the relationships of the coordinates for the corresponding nodes can be represented by

$$\begin{cases}x_i^2=\alpha x_i^1,\\ \theta_i^2=\alpha\theta_i^1.\end{cases} \quad (7)$$

The matrix $\boldsymbol{B}$ in Eq.(3) can be decomposed as

$$\boldsymbol{B}=\overline{\boldsymbol{B}}+\overline{\overline{\boldsymbol{B}}}=\begin{bmatrix}\dfrac{\partial N_i}{\partial x} & 0 & 0\\ 0 & \dfrac{1}{r}\dfrac{\partial N_i}{\partial \theta} & 0\\ \dfrac{1}{r}\dfrac{\partial N_i}{\partial \theta} & \dfrac{\partial N_i}{\partial x} & 0\end{bmatrix}+\begin{bmatrix}0 & 0 & 0\\ 0 & 0 & -\dfrac{N_i}{r}\\ 0 & 0 & 0\end{bmatrix}. \quad (8)$$

Therefore, from Eqs.(7) and (8), the matrices $\overline{\boldsymbol{B}}$ and $\overline{\overline{\boldsymbol{B}}}$ for element 1 and element 2 have the following relationships:

$$\begin{cases}\overline{\boldsymbol{B}}_2=\overline{\boldsymbol{B}}_1/\alpha,\\ \overline{\overline{\boldsymbol{B}}}_2=\overline{\overline{\boldsymbol{B}}}_1,\end{cases} \quad (9)$$

and the relationships of the Jacobian matrix are:

$$\begin{cases}\boldsymbol{J}_2=\alpha\boldsymbol{J}_1,\\ \boldsymbol{J}_2^{-1}=\boldsymbol{J}_1^{-1}/\alpha,\\ \det|\boldsymbol{J}_2|=\alpha^2\det|\boldsymbol{J}_1|.\end{cases} \quad (10)$$

By substituting Eq.(8) into Eq.(4), the stiffness matrix $\boldsymbol{K}$ becomes as

$$\boldsymbol{K}=\aleph^{*}+\aleph^{**}+\aleph^{***},$$

where

$$\aleph^{*}=t\int_{-1}^{1}\int_{-1}^{1}\overline{\boldsymbol{B}}^{\mathrm{T}}\boldsymbol{D}\overline{\boldsymbol{B}}\det|\boldsymbol{J}|\,r\mathrm{d}\xi\mathrm{d}\eta,$$

$$\aleph^{**}=t\int_{-1}^{1}\int_{-1}^{1}(\overline{\overline{\boldsymbol{B}}}^{\mathrm{T}}\boldsymbol{D}\overline{\boldsymbol{B}}+\overline{\boldsymbol{B}}^{\mathrm{T}}\boldsymbol{D}\overline{\overline{\boldsymbol{B}}})\det|\boldsymbol{J}|\,r\mathrm{d}\xi\mathrm{d}\eta,$$

$$\aleph^{***}=t\int_{-1}^{1}\int_{-1}^{1}\overline{\overline{\boldsymbol{B}}}^{\mathrm{T}}\boldsymbol{D}\overline{\overline{\boldsymbol{B}}}\det|\boldsymbol{J}|\,r\mathrm{d}\xi\mathrm{d}\eta.$$

The relationships of matrices $\aleph^{*}$, $\aleph^{**}$ and $\aleph^{***}$ for element 1 and element 2 are derived from Eqs.(4), (6) and (9). Then, the following equation can be acquired to reflex the above-mentioned relation:

$$\boldsymbol{K}_2=\aleph_1^{*}+\alpha\aleph_1^{**}+\alpha^2\aleph_1^{***}. \quad (11)$$

SUPER ELEMENT FORMULATION

The element mesh around a singularity point is shown in Fig.2. These elements are similar to each other. The inner-layer element to the adjacent outer-layer element is designed with the ratio α. The stiffness of the outmost element may be expressed as

$$\boldsymbol{K}_1=\aleph_1^{*}+\aleph_1^{**}+\aleph_1^{***}$$
$$=\begin{bmatrix}\boldsymbol{k}_1^{*} & \boldsymbol{k}_2^{*} & \boldsymbol{k}_3^{*}\\ \boldsymbol{k}_2^{*\mathrm{T}} & \boldsymbol{k}_4^{*} & \boldsymbol{k}_5^{*}\\ \boldsymbol{k}_3^{*\mathrm{T}} & \boldsymbol{k}_5^{*\mathrm{T}} & \boldsymbol{k}_6^{*}\end{bmatrix}+\begin{bmatrix}\boldsymbol{k}_1^{**} & \boldsymbol{k}_2^{**} & \boldsymbol{k}_3^{**}\\ \boldsymbol{k}_2^{**\mathrm{T}} & \boldsymbol{k}_4^{**} & \boldsymbol{k}_5^{**}\\ \boldsymbol{k}_3^{**\mathrm{T}} & \boldsymbol{k}_5^{**\mathrm{T}} & \boldsymbol{k}_6^{**}\end{bmatrix}+\begin{bmatrix}0 & 0 & 0\\ 0 & 0 & 0\\ 0 & 0 & \boldsymbol{k}_6^{***}\end{bmatrix}. \quad (12)$$

Then, the stiffness matrix for the m-layer element is

$$\boldsymbol{K}_m=\aleph_1^{*}+\alpha^{m-1}\aleph_1^{**}+\alpha^{2(m-1)}\aleph_1^{***}.$$

For the condensation purpose, the internal displacements at the jointed boundary of the elements are eliminated as follows:

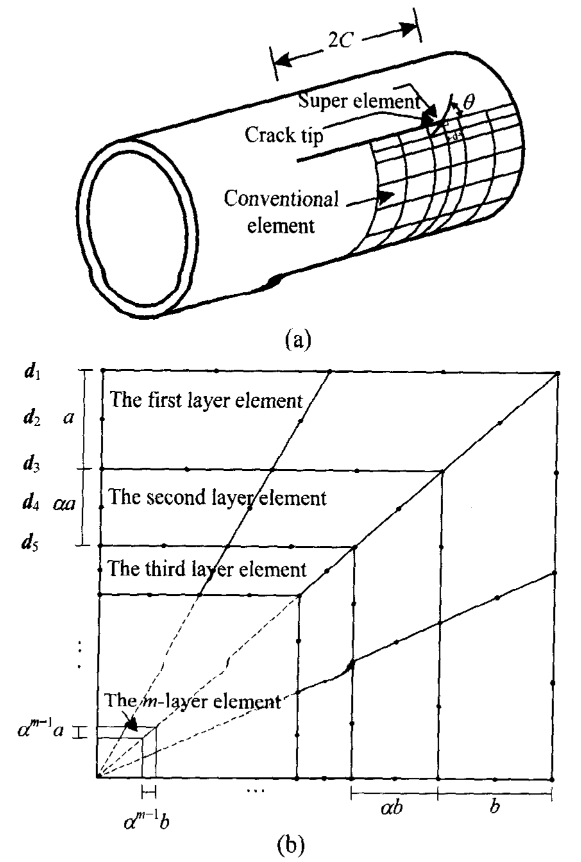

Fig.2 Mesh for the cylindrical pressure vessel around through-wall tip. (a) Cylindrical coordinate; (b) Plane projection

$$\begin{bmatrix} k_1 & k_2 & k_3 & 0 & 0 \\ k_2^{\mathrm{T}} & k_4 & k_5 & 0 & 0 \\ k_3^{\mathrm{T}} & k_5^{\mathrm{T}} & k_6+\kappa_1 & \kappa_2 & \kappa_3 \\ 0 & 0 & \kappa_2^{\mathrm{T}} & \kappa_4 & \kappa_5 \\ 0 & 0 & \kappa_3^{\mathrm{T}} & \kappa_5^{\mathrm{T}} & \kappa_6 \end{bmatrix} \begin{Bmatrix} d_1 \\ d_2 \\ d_3 \\ d_4 \\ d_5 \end{Bmatrix} = \begin{Bmatrix} p_1 \\ p_2 \\ p_3 \\ p_4 \\ p_5 \end{Bmatrix}. \quad (13)$$

The column matrices of $\boldsymbol{d}_i$ and $\boldsymbol{p}_i$ are the representations of displacements and forces at nodes respectively. The elimination of the displacements $\boldsymbol{d}_3$ and $\boldsymbol{d}_4$ is along the joint boundary. Eq.(13) is rearranged as:

$$\begin{bmatrix} k_1 & k_2 & 0 & \cdots & k_3 & 0 \\ k_2^{\mathrm{T}} & k_4 & 0 & \cdots & k_5 & 0 \\ 0 & 0 & \kappa_6 & \cdots & \kappa_3^{\mathrm{T}} & \kappa_5^{\mathrm{T}} \\ \vdots & \vdots & \vdots & \cdots & \vdots & \vdots \\ k_3^{\mathrm{T}} & k_5^{\mathrm{T}} & \kappa_3 & \cdots & k_6+\kappa_1 & \kappa_2 \\ 0 & 0 & \kappa_5 & \cdots & \kappa_2^{\mathrm{T}} & \kappa_4 \end{bmatrix} \begin{Bmatrix} d_1 \\ d_2 \\ d_5 \\ \vdots \\ d_3 \\ d_4 \end{Bmatrix} = \begin{Bmatrix} p_1 \\ p_2 \\ p_5 \\ \vdots \\ p_3 \\ p_4 \end{Bmatrix}. \quad (14)$$

Let

$$\begin{bmatrix} (\boldsymbol{K}_{\mathrm{II}})_{3\times3} & (\boldsymbol{K}_{\mathrm{IE}})_{3\times2} \\ (\boldsymbol{K}_{\mathrm{EI}})_{2\times3} & (\boldsymbol{K}_{\mathrm{EE}})_{2\times2} \end{bmatrix} \begin{Bmatrix} (\boldsymbol{Y}_{\mathrm{I}})_{3\times1} \\ (\boldsymbol{Y}_{\mathrm{E}})_{2\times1} \end{Bmatrix} = \begin{Bmatrix} (\boldsymbol{P}_{\mathrm{I}})_{3\times1} \\ (\boldsymbol{P}_{\mathrm{E}})_{2\times1} \end{Bmatrix}. \quad (15)$$

Eq.(15) can be shown as:

$$\boldsymbol{K}_{\mathrm{I}}^{*}\boldsymbol{Y}_{\mathrm{I}}^{*} = \boldsymbol{P}_{\mathrm{I}}^{*}, \quad (16)$$

and then,

$$\boldsymbol{Y}_{\mathrm{E}} = \boldsymbol{K}_{\mathrm{EE}}^{-1}(\boldsymbol{P}_{\mathrm{E}} - \boldsymbol{K}_{\mathrm{EI}}\boldsymbol{Y}_{\mathrm{I}}), \quad (17)$$

and condensed form of Eq.(15) is shown as:

$$(\boldsymbol{K}_{\mathrm{II}} - \boldsymbol{K}_{\mathrm{IE}}\boldsymbol{K}_{\mathrm{EE}}^{-1}\boldsymbol{K}_{\mathrm{EI}})\boldsymbol{Y}_{\mathrm{I}} = \boldsymbol{P}_{\mathrm{I}} - \boldsymbol{K}_{\mathrm{IE}}\boldsymbol{K}_{\mathrm{EE}}^{-1}\boldsymbol{P}_{\mathrm{E}}, \quad (18)$$

where the transformation matrix $\boldsymbol{T}$ is defined as

$$\boldsymbol{T} = \begin{bmatrix} \boldsymbol{I} \\ -\boldsymbol{K}_{\mathrm{IE}}\boldsymbol{K}_{\mathrm{EE}}^{-1} \end{bmatrix},$$

in which $\boldsymbol{I}$ is an identity matrix. Eq.(18) can be rewritten as:

$$\boldsymbol{T}^{\mathrm{T}}\boldsymbol{K}_{\mathrm{I}}^{*}\boldsymbol{T}\boldsymbol{Y}_{\mathrm{I}} = \boldsymbol{T}^{\mathrm{T}}\boldsymbol{P}_{\mathrm{I}}^{*}. \quad (19)$$

When using layer-by-layer approach to the singular point, Eq.(19) is utilized to formulate a final stiffness matrix for analysis.

NUMERICAL EXAMPLE

The pressure vessel is designed as an inside radius of 25 cm and a wall thickness of 1.2 cm to withstand an internal pressure of 10 MPa. The vessel is made using a material with Young's modulus E=206.78 GPa and Poisson's ratio υ=0.3. The size of through-thickness crack varies from 0.001 cm to 2.6 cm. It is used in the numerical test to calculate the stress intensity factor. The super element is generated by α=0.5. Three cases are performed. The first is for an axial crack, the second for a peripheral crack and the third for an arbitrary orientation crack. The proposed finite element algorithms present a very good agreement with the result founded by Sih (1977). These results are shown in Figs.3~5. The excellence of convergent characteristics in numerical calculation is shown in Fig.6, where the normalized stress intensity is defined as stress intensity factor divided by extensional stresses through the thickness. The results show that the normalized stress intensity factors are converged to a value at the ratio of the crack length to the radius approaching 10^{-2} for these three cases. The ratio of stress values for crack versus without crack around crack tip converges to 3.5 shown in Fig.7. It is realized that the kinked crack problem is very complicated (Dutta *et al.*, 1990) because of the existence of two singular points at a close distance such that the general solutions are not available at cylindrical shell.

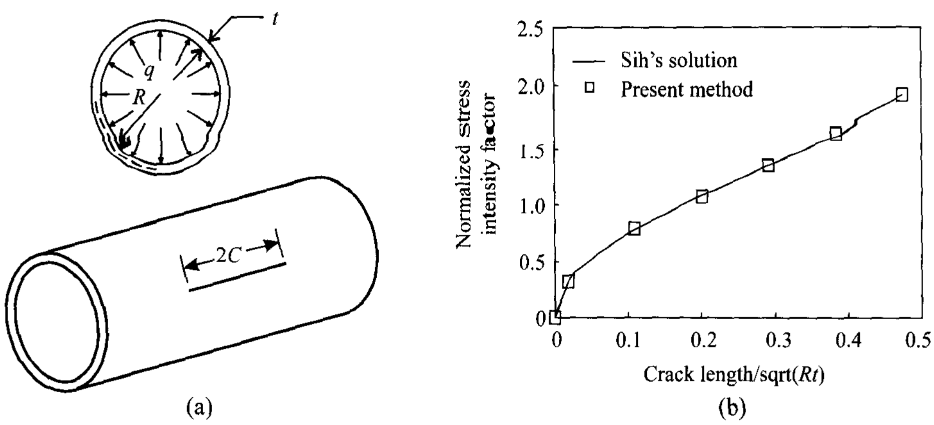

Fig.3 For axial crack stress intensity factor versus crack length/$\sqrt{Rt}$, r=c/2
(a) Internal force of pipe and crack location; (b) Comparison sheet

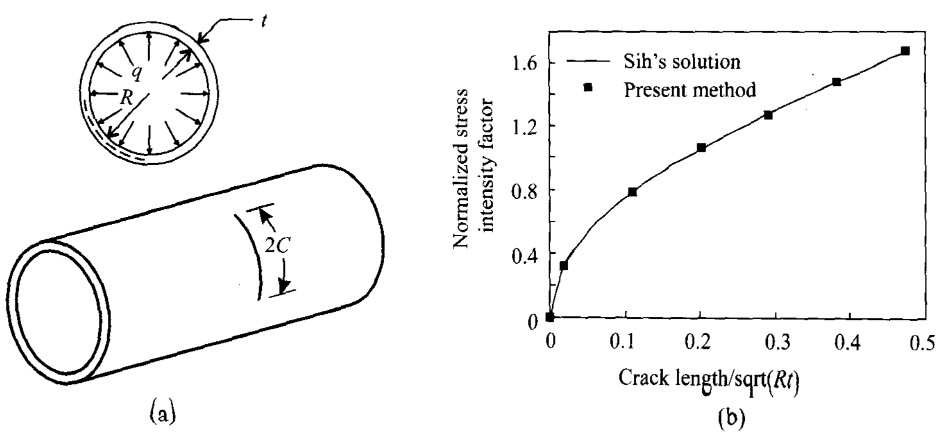

Fig.4 For peripheral crack stress intensity factor versus crack length/$\sqrt{Rt}$, r=c/2
(a) Internal force of pipe and crack location; (b) Comparison sheet

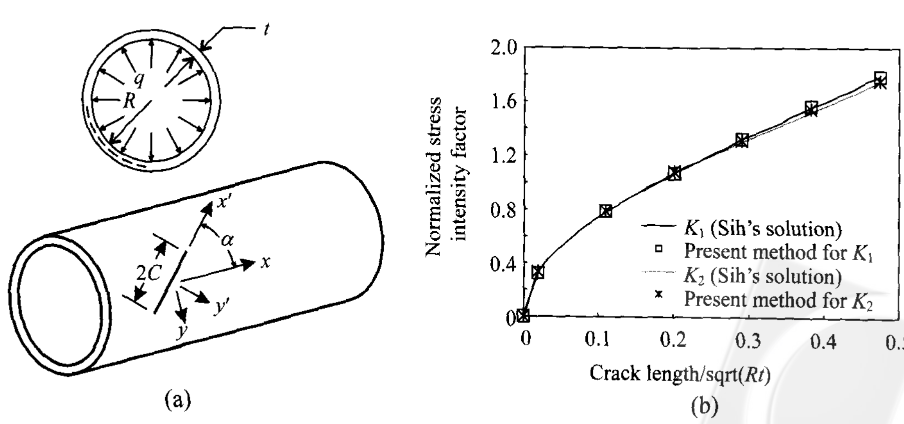

Fig.5 For an arbitrary orientation crack stress intensity factor versus crack length/$\sqrt{Rt}$, r=c/2
(a) Internal force of pipe and crack location; (b) Comparison sheet

For an example, in (Dutta *et al.*, 1990) the calculations give the same result as that of (Dutta *et al.*, 1990) which indicated in Fig.8. Nevertheless, the proposed technique is more versatile in singular problems.

DISCUSSION

The failure of pressure vessel may be caused by unstable propagation of an existing crack. Therefore the tolerance of vessel structure flaws has to be considered. The fracture mechanics are feasible tool to evaluate the integrity of the pressure vessels with crack. In ordinary fracture problems, quarter-point element (QPE) is often used because of its simplicity. In this QPE method, strains are represented as a constant plus a term proportional to singular order −1/2. The variation of stress filed is dependent on the element size. Accordingly, the optimum size of the element used has to be selected with care (Szilard, 1974). For improving this technique, the transient element (Tani *et al.*, 2000) by special placement of nodes in cooperation with QPE is suggested for better solutions. The alternative methods without invoking special placement of nodes are also developed. Such hybrid element (Zhao *et al.*, 1999) is designed by using the knowledge of the strain or stress filed and proper singularity order. Nevertheless, these techniques have the similar restriction and valid only for problems with a known stress singularity. By the application of the characteristic of similar elements, the proposed approach provides a merit to skip over the difficulty of knowing stress singularity in advance in element design. Since the calculation process is formulated by the condensation of a geometric series of similar element, the mathematical simplicity can make the FEM to be programmed easily and economically.

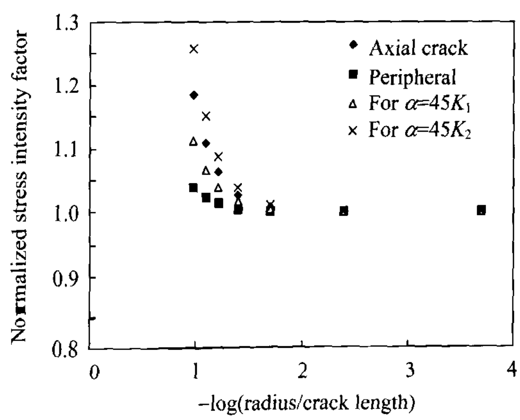

Fig.6 Normalized stress intensity factor versus −log(radius/crack length)

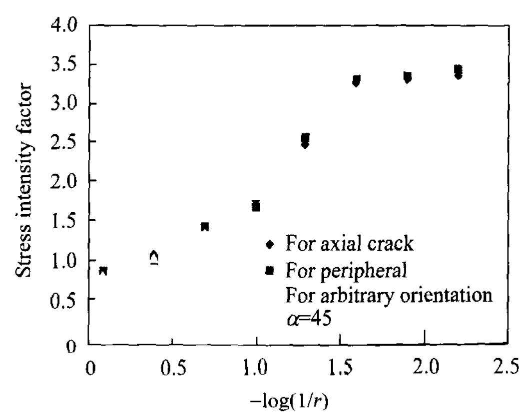

Fig.7 Convergence of the present method

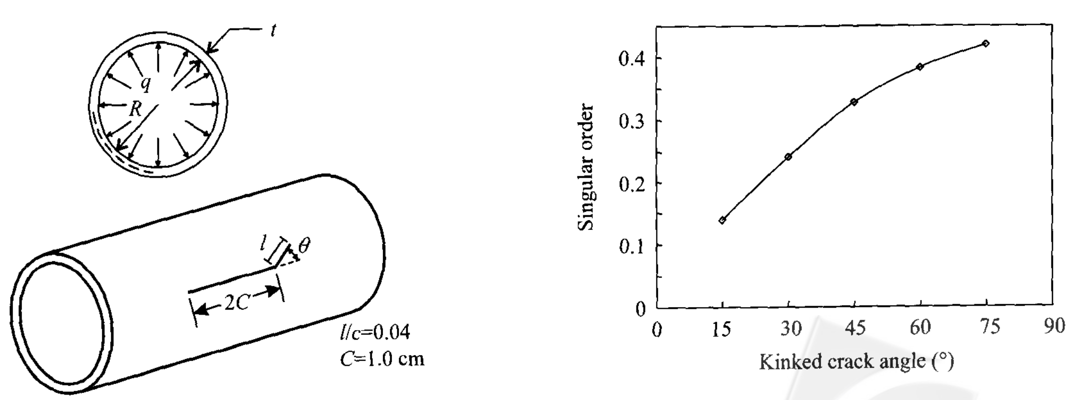

(a) (b)

Fig.8 Singular order at the kinked crack of cylindrical pressure vessel
(a) Internal force of pipe and crack location; (b) Comparison sheet

CONCLUSION

The stress at the crack tip changes rapidly. A group of small elements surrounding the crack tip is a warrant for better solution in finite element calculation. By merely using the characteristic properties of shell element and the approach of matrix condensation, the elements at crack tip can easily be subdivided to arbitrarily small. Thus, the special element with the necessity of knowledge of stress field around the crack tip is not required in the fracture analysis. Since the difficulty for determining the singular order in advance of FEM calculation always exists for most of the cases, the proposed method provides a valid approach for general solution. Beside this advantage, economy in computer memory and programming process is also shown.

References

Ainsworth, R.A., Ruggles, M.B., Takahashi, Y., 1992. Flaw assessment procedure for high-temperature reactor components. *J. Pressure Vessel Technology, Trans. ASME*, **114**:166-170.

Anderson, T.L., 1991. Fracture Mechanics: Fundamentals and Applications. CRC Press, Boca Raton.

Atluri, S.N., 1986. Computation Methods in the Mechanics of Fracture. North-Holland, Amsterdam.

Chen, W.H., Lin, H.C., 1985. Flutter analysis of thin cracked panels using the finite element method. *AIAA J.*, **23**:795-801.

Cook, R.D., Malkus, D.S., Plesha, M.E., 1989. Concepts and Applications of Finite Element Analysis. John Wiley and Sons.

Dutta, B.K., Maiti, S.K., Kakodkar, A., 1990. On the use of one point and two point's singularity elements in the analysis of kinked crack. *Int. J. Numeral Meth. Eng.*, **29**(7):1487-1499. [doi:10.1002/ nme.1620290708]

Folias, E.S., 1999. Failure correlation between cylindrical pressurized vessels and flat plates. *Int. J. Pressure Vessels and Piping*, **76**(11):803-811. [doi:10.1016/S0308-0161(99)00045-9]

Go, C.G., Chen, G.C., 1992. On the use of an infinitely small element for the three-dimensional problem of stress singularity. *Computers & Structures*, **45**(1):25-30. [doi:10.1016/0045-7949(92)90341-V]

Go, C.G., Lin, Y.S., 1991. Infinitely small element for the problem of stress singularity. *Computers & Structures*, **37**:547-551.

Go, C.G., Lin, Y.S., 1994. Infinitely small element for the dynamic problem of a crack beam. *Eng. Fracture Mech.*, **48**(4):475-482. [doi:10.1016/0013-7944(94)90202-X]

Go, C.G., Lin, C.I., Lin, Y.S., Wu, S.H., 1998. Formulation of a super-element for the dynamic problem of a cracked plate. *Commun. Numer. Meth. Engng.*, **14**(12):1143-1154. [doi:10.1002/(SICI)1099-0887(199812)14:12<1143::AID-CNM215>3.0.CO;2-J]

Hooton, D.G., Tomkins, B., 1996. Development of structural integrity criteria for austenitic components. *Int. J. Pressure Vessels and Piping*, **65**(3):311-316. [doi:10.1016/0308-0161(94)00142-6]

JHGPA (Inc. Japan Hydraulic Gate and Penstock Association), 1986. Technical Standards for Gates and Penstock.

Knott, J.F., 1973. Fundamentals of Fracture Mechanics. Halsted Press.

Kobayashi, A.S., 1973. Experimental Techniques in Fracture Mechanics. SESA (Society for Experimental Stress Analysis) Monographs, No. 1 and 2. Westport, CT.

Lakshminarayana, H.V., Murthy, M.V.V., Srinath, L.S., 1982. On an analytical-numerical procedure for the analysis of cylindrical shell with arbitrary oriented cracks. *Int. J. Fracture*, **19**(4):257-275. [doi:10.1007/BF00012483]

Le Van, A., Royer, J., 1986. Integral equations for three-dimensional problems. *Int. J. Fracture*, **31**(2):125-142. [doi:10.1007/BF00018918]

Lynn, P.P., Ingraffen, A.R., 1978. Transition elements to be used with quarter point crack tip elements method. *Int. J. Numeral Meth. Eng.*, **12**(6):1031-1036. [doi:10.1002/nme.1620120612]

Minnetyan, L., Chamis, C.C., 1999. Damage tolerance of large shell structures. *J. Pressure Vessel Technology, Trans. ASME*, **121**:188-195.

Mutri, V., Valliappan, S., Lee, I.K., 1985. Stress Intensity factor using Quarter Point Element. *ASCE J. Eng. Mech. Div.*, **111**(2):203-217.

Nichols, R.W., 1987. Pressure Vessel Codes and Standards. Elsevier Applied Science Publisher Ltd.

Pilkey, W.D., 1994. Formulas for Stress, Strain, and Structural Matrices. John Wiley and Sons, Inc., p.117.

Shephard, M.S., Gallagher, R.H., Abel, J.F., 1981. Finite element solution to point-load problems. *ASCE J. Eng. Mech. Div.*, **107**(5):839-850.

Sih, G.C., 1977. Mechanics of Fracture: Plates and Shells with Cracks—A Collection of Stress Intensity Factor Solutions for Cracks in Plates and Shells (Vol. 3). Noordhoff International Publishing.

Song, C., 2004. A super-element for crack analysis in the time domain. *Int. J. Numeral Meth. Eng.*, **61**(8):1332-1357. [doi:10.1002/nme.1117]

Szilard, R., 1974. Theory and Analysis of Plates, Classical and Numerical Methods. Prentice-Hall, Inc., p.3.

Tani, K., Yamada, T., Kawase, Y., 2000. Error estimation for transient finite element method using edge elements. *IEEE Transactions on Magnetics, 12th Conference of the Computation of Electromagnetic Fields*, **36**(4):1488-1491.

Timoshenko, S., 1955. Strength of Materials. Part I (3rd Ed.). D. Van Nostrand Co., New York, USA, p.370.

Timoshenko, S., Woinowsky-Krieger, S., 1959. Theory of Plates and Shells (2nd Ed.). McGraw-Hill, London, UK, p.431.

Ugural, A.C., 1981. Stresses in PLATES and Shells. McGraw-Hill, Inc.

Zhao, J., Hoa, S.V., Xiao, X.R., Hanna, I., 1999. Global/local approach using partial hybrid finite element analysis of stress fields in laminated composites with mid-plane delamination under bending. *J. Reinforced Plastics and Composites*, **18**(9):827-843.

Zheng, J.Y., Chen, Y.J., Deng, G.D., Sun, G.Y., Hu, Y.L., Li, Q.M., 2006. Dynamic elastic response of an infinite discrete multi-layered cylindrical shell subjected to uniformly distributed pressure pulse. *Int. J. Impact Engineering*, **32**(11):1800-1827. [doi:10.1016/j.ijimpeng.2005.05.011]